Cement and Concrete Composites 104 (2019) 103410

Contents lists available at ScienceDirect

Cement and Concrete Composites

journal homepage: www.elsevier.com/locate/cemconcomp

Characterization and pozzolanic properties of sewage sludge ashes (SSA) by electrical conductivity

Priscilla de Azevedo Basto[a], Holmer Savastano Junior[b], Antonio Acacio de Melo Neto[a,*]

[a] Laboratório de Tecnologia dos Aglomerantes (LabTag), Departamento de Engenharia Civil e Ambiental, Universidade Federal de Pernambuco, Brazil
[b] Department of Biosystems Engineering, University of São Paulo, Brazil

ARTICLE INFO

Keywords:
Sewage sludge ash
Pozzolanic reactions
Conductivity
Compressive strength

ABSTRACT

Urbanization and continuing population and industrial growth have led to the intensification of management issues related to residues of wastewater treatment. To reduce sludge storage and carbon dioxide emissions resulting from Portland cement production, the pozzolanic activity of sewage sludge ash (SSA) was studied as a supplementary cementitious material (SCM). The SSAs that calcined in the temperature range of 600–900 °C were characterized by XRD, XRF, and laser diffraction. The pozzolanic reaction was monitored by an electrical conductivity measurement test, which demonstrated that the decrease in conductivity of an unsaturated pozzolan/calcium hydroxide suspension is correlated with the consumption of $Ca(OH)_2$ during 1000 s. The results indicated that the calcination of sewage sludge at 600 °C is the most adequate for use as a pozzolan as it obtained a higher loss in conductivity (88.3%) and consumed less energy during the incineration process. A good correspondence was found between the mortar compressive strength test and the conductivity test, and both indicated that pozzolanicity decreases with temperature. Therefore, this method was found to be effective and hence can be used as a rapid and simple test for the pozzolanic activity evaluation of SSA.

1. Introduction

The construction industry is one of the major consumers of non-renewable natural resources and energy. Additionally, construction expansion increases carbon dioxide (CO_2) emissions caused by cement production, which impacts the environment by contributing to climate change and the raising of the Earth's surface temperature. These emissions are generated by the calcination reaction that produces clinker, a major component of cement, and the combustion of fossil fuels used to produce energy. Almost 750 kg of CO_2 per ton of cementitious products are produced by these two factors in conjunction, and they contribute to approximately 8% of global carbon dioxide emissions [1,2]. To mitigate CO_2 emissions, several strategies have been studied, for example, the use of alternative fuels and the production of cement with lower ratios of clinker. The last mentioned option is the most viable short-term alternative, and can be achieved by increasing the development of recycled and secondary materials as sustainable construction materials [3,4].

Constant population growth, urbanization, and industrial and technological development drastically increase the volume of generated wastewater and, consequently, sewage sludge. Globally, according to the empirical data compiled from a variety of sources by AQUASTAT [5], 311.6 km^3 of municipal wastewater is produced annually, of which 60% (187.4 km^3 $year^{-1}$) is treated. Despite the portion of sludge that is used in wastewater treatment plants (WWTP), a huge quantity still needs to be removed. Together, the European Union, the United States, China, Japan, Canada, Brazil, Australia, and New Zealand produce approximately 22,000 dry metric tons of sewage sludge [6,7]. Thus, the treatment facility deals with complex and costly management of residues [8–10]. Although sludge processing represents 45–50% of the total operating costs at the wastewater treatment plant, the planning and execution of disposal have been continuously neglected in developing countries [10–12].

Controlled incineration is widely used as a disposal alternative for sewage sludge due to the difficulties of maintaining landfills and restrictions in agricultural use [9,13]. The reuse and recycling of sewage sludge ash (SSA) in construction has great potential and several possibilities have been explored, namely, ceramic products, road pavements, soil stabilization, lightweight aggregate, mineral addition, mortar, and concrete [4,14–18]. Of these examples, concrete is preferable because it stabilizes heavy metals and adds higher value. However, the origin of wastewater, the type of treatment used, and the incineration system,

* Corresponding author. Universidade Federal de Pernambuco, Center of Technology and Geosciences (CTG) - Federal University of Pernambuco, Av. da Arquitetura, s/n - Cidade Universitária, Recife, PE, 50740-550, Brazil.
E-mail addresses: priscilla.basto@ufpe.br (P. de Azevedo Basto), holmersj@usp.br (H. Savastano Junior), antonio.meloneto@ufpe.br (A.A. de Melo Neto).

https://doi.org/10.1016/j.cemconcomp.2019.103410
Received 21 April 2019; Received in revised form 31 July 2019; Accepted 3 September 2019
Available online 04 September 2019
0958-9465/

may cause variations in SSA performance. Therefore, it is recommended that the material be studied before use [13,17,19].

Because the hydration of cementitious materials becomes an even more complex process in the presence of a varied range of mineral additions available on the market, it was not feasible to create a model capable of fully elucidating the pozzolanic activity. Several methods have been proposed to evaluate the pozzolanic reactivity, usually based on the principle of the interaction between calcium hydroxide and pozzolans [20–23]. In these methods, physical and chemical properties are considered, and qualitative and quantitative evaluations may also be conducted.

Based on the studies conducted by Raask and Bhaskar [24], Lúxan et al. [25] created a rapid and indirect method to determine the potential pozzolanicity of natural products. The principle of this method was to decrease the conductivity induced through the consumption of portlandite by a pozzolan in the water solution. The variation in electrical conductivity in a calcium hydroxide (CH) saturated solution was measured over 120 s. However, due to the fact that $Ca(OH)_2$ is slow to dissolve and reach saturation, as well as the insufficient test time for fly ash evaluation, Payá et al. [26] presented a methodology that uses a calcium hydroxide unsaturated solution to determine the percentage loss in conductivity (% LC) of low-lime fly ash at 100, 1000, and 10000 s.

This study aims to characterize and monitor pozzolanic reactions of sewage sludge ash that has the potential to be incorporated into cementitious composites. In this regard, the loss in conductivity using Payá's method has been verified using the average of five conductivity curves. This approach enables the investigation of the method's repeatability and aims to minimize errors. Sewage sludge ash produced with four calcination temperatures were evaluated and their properties were compared with metakaolin, which is a high-performance pozzolan.

2. Materials and methods

2.1. Materials

The sewage sludge used was generated by the Mangueira Wastewater Treatment Plant and collected from the Upflow Anaerobic Sludge Blanket (UASB) reactor in a liquid state. The wastewater was mainly composed of domestic sewage and the reactor detention time was 8 h for an average daily flow of 31.11 L/s. Mangueira WWTP is located in the West Zone of the city of Recife, the capital of Pernambuco State, which is the ninth most populous city in Brazil, with approximately 1.7 million inhabitants. Before calcining, most of the water contained in the sludge was removed using a 45 μm mesh sieve. The retained material was sun-dried for 6 days and dried at 110 °C for 24 h. Next, to guarantee homogeneous diffusion of heat during calcination, the dried sewage sludge was ground for 20 min in a ball mill.

Besides sewage sludge, the materials used in the pozzolanic activity evaluation tests were calcium hydroxide p. a. (≥ 95%) and metakaolin. The chemical composition and the loss on ignition (LOI) of the anhydrous samples, measured by semiquantitative X-ray fluorescence (XRF) spectrometry, are presented in Table 1. The dried sewage sludge (DSS) presented a high LOI when compared to metakaolin. This occurs due to the considerable content of organic matter in DSS. Thus, the calcination process may improve the properties of the material by eliminating this undesirable matter. Table 2 presents the particle size distribution by laser diffraction, the Blaine fineness, and the density. The volume particle size distribution is described by D-values (D_{10}, D_{50}, and D_{90}), which are the percentage of particles smaller than the calculated diameter based on the results from the sieving analysis. The D_{mean} refers to the volume mean diameter (de Brouckere mean) and represents the particle size of the bulk of the sample volume.

The fine aggregates consist of quartz sand with a specific gravity of 2.64 g/cm^3 and a fineness modulus of 2.14. This material was used to produce five mortars with a calcium hydroxide to sand ratio of 1:9.

Table 1
Chemical composition in oxide content (%) of dried sewage sludge (DSS), calcium hydroxide (CH), and metakaolin (MK) samples.

Sample	DSS	CH	MK
Oxide	Mass content (%)		
SiO_2	39.02	0.49	50.27
Al_2O_3	16.02	0.32	42.80
Fe_2O_3	9.68	0.09	3.61
CaO	6.62	72.47	0.08
P_2O_5	5.42	0.24	0.37
MgO	2.21	0.58	0.22
K_2O	1.67	0.05	0.22
Na_2O	0.80	–	0.02
CuO	0.12	–	–
MnO	0.06	–	–
NiO	0.06	–	–
LOI	18.33	25.76	2.40

Table 2
Particle size (D_{10}, D_{50}, D_{90}, D_{mean}), Blaine fineness, and density of dried sewage sludge, calcium hydroxide, and metakaolin samples.

Sample	DSS	CH	MK
D_{10}	8.994	1.795	2.463
D_{50}	39.627	9.911	16.050
D_{90}	92.373	22.163	52.714
D_{mean}	45.955	11.161	22.147
Density (g/cm^3)	2.73	2.33	2.56
Blaine fineness (m^2/kg)	676.96	1187.55	2348.97

2.2. Preparation and characterization of sewage sludge ash

The calcination temperature was established on the basis of results published in the literature [21,27,28] and ranged from 600 °C to 900 °C. The studies evidenced that the minimum temperature for the disappearance of undesirable organic matter is 500 °C and the maximum temperature for avoiding loss of pozzolanic properties is 900 °C. The ash was designated according to the calcination temperature as SSA600, SSA700, SSA800, and SSA900. Each sample was heated from room temperature up to the designated temperatures (600, 700, 800, and 900 °C) in an electrical muffle with a heating rate of 10 °C/min. The temperature was maintained for 180 min and then cooled down to room temperature.

The parameters selected to characterize the different SSA samples were their chemical and mineralogical compositions, specific gravity, specific surface area, and particle size distribution. Finally, the pozzolanic activity was also evaluated for each sample.

The microstructure was assessed using: X-ray fluorescence spectrometry (XRF) (Rigaku ZSX Primus II spectrometer) by semi-quantitative analysis in a pressed pellet; the laser diffraction particle size (Mastersizer 2000 with the dispersion unit Hydro 2000MU, Malvern Instruments) with a measuring range from 0.02 to 2000 μm; X-ray diffraction (XRD) (Rigaku D/max-2200 diffractometer) from 2 to 70° 2θ with a 0.02° 2θ step size, a time per step of 1 s, and Cu Kα radiation operating at 20 mA and 40 kV.

2.3. Evaluation of the pozzolanic reaction

The pozzolanic activity was measured by a compressive strength test and an electrical conductivity test. In the first method, the compressive strength was assessed on mortar cylinders (50 mm diameter x 100 mm height) composed of 1 part calcium hydroxide (104 g), 9 parts sand mass (936 g), and a quantity of pozzolan equivalent to double that of the volume of CH. The mass of pozzolan was obtained by the

following equation:

$$m_{poz} = 2 \cdot \frac{\delta_{poz}}{\delta_{CH}} \cdot 104 \quad (1)$$

where m_{poz}, δ_{poz}, δ_{CH} are respectively the mass of the pozzolan, the density of the pozzolan, and the density of the calcium hydroxide. The equivalent mass ensures that the quantity of any pozzolanic material tested would be suited to consume the indicated mass of calcium hydroxide. The water-binder ratio (w/b) should be enough to reach a constant flow of (225 ± 5) mm. After one day of curing at room temperature, the samples were kept in molds in a drying oven at 55 °C for 6 days, as is stated in the Brazilian standard [29]. The thermal cure is used to reach a higher consumption of CH and to increase the mechanical behavior of the pastes. After 7 days, the samples were removed from the oven 1 h before the mechanical test and rested at room temperature. Then they were unmolded and the compressive strengths were measured as the average of three specimens using a manual hydraulic testing machine *Solotest* 100/20 TON. A sample passed this test if it achieved a minimum of 6 MPa of compressive strength [30].

For the second method, the loss in conductivity of a pozzolan added to an unsaturated calcium hydroxide solution (pozzolan/calcium hydroxide ratio of 1:0.04) at 100 and 1000 s was evaluated, based on the method of Payá et al. [26]. A Digimed DM-32 v.2.0 conductivity meter and a Digimed stainless steel conductivity cell model DMC-001 XTX were utilized for the measurements. The data was acquired and stored by a Raspberry Pi 3 connected to the conductivity meter. The test used a glass beaker, a rubber stopper to prevent carbonation of the solution, and a magnetic stirrer that allowed for the adjustment of the base plate temperature and stirring rate. To analyze the method's repeatability, each sample was tested 5 times and the average data for each second was used to create the average conductivity curve used in the comparative study.

Initially, a volume of deionized water that was enough to conduct all repetitions (1050 L) was heated up to (60 ± 1) °C and, after reaching this temperature, CH was added (840 mg). The selection of this temperature was derived from the initial exothermic temperature of Portland cement hydration, and the solution concentration was indicated by Payá et al. [26]. The vessel was sealed, and the solution was stirred at 700 rpm for 1 h. The initial conductivity ranged from 5.55 mS/cm to 5.93 mS/cm. Then, the solution was transferred to a beaker (200 mL) which was sealed with a rubber stopper plugged tightly, the conductivity cell and thermometer were attached, and the pozzolan (4 g) was added to the calcium hydroxide-water suspension. The conductivity of this solution was measured every second for 1000 s. Some tested pozzolans presented a significant contribution to electrical conductivity when added to deionized water due to the presence of water-soluble components. The conductivity obtained in pozzolan aqueous suspensions $(C_{poz})_t$ was subtracted from the pozzolan/CH suspension $(C_{pozch})_t$ to determine the absolute loss in conductivity $(C_{poza})_t$. Finally, the relative loss in conductivity for a given time $(\%LC)_t$ was determined by the ratio between the initial conductivity (C_0) subtracted by $(C_{poza})_t$, and the initial conductivity, as indicated in Equation (2).

$$(\%LC)_t = \frac{C_0 - (C_{poza})_t}{C_0} \cdot 100 \quad (2)$$

3. Results

3.1. Sewage sludge ash characterization

Table 3 presents the oxide content in the sewage sludge ash by X-ray fluorescence analysis. Both metakaolin and the sewage ash samples are mainly composed of SiO_2. Silicon amorphous is the main component responsible for the pozzolanicity in SCM, and it is highly indicative of SSA pozzolanic reactivity. The next most abundant components were Al_2O_3, Fe_2O_3, and CaO, coinciding with results observed in other chemical analyses [19,27,31–48]. The significant levels of these oxides may be derived from the use of alumina salt, ferric salt, and lime in the domestic wastewater treatment process, respectively. The significant percentage of P_2O_5 may be resultant of its presence in dishwashing liquid compositions. Furthermore, it was observed that the variation of the calcination temperature within the studied range did not have a remarkable influence on the percentage of oxides. Loss on ignition was within the range obtained by other authors (1.80–8.35%) [27,31,33–37,39,41,42,45–47] and has been found to decrease with increasing temperature.

Sewage sludge ash density varied from 2.58 to 2.63 g/cm^3, which is lower than the DSS, as listed in Table 4. Therefore, it was concluded that these materials have a density comparable to natural sand and metakaolin. It was observed that from 600 to 800 °C sewage sludge calcination promoted a decrease in the specific gravity, but an increase thereof at 900 °C. Presumably, this increase is related to a reduction in pore space caused by the vitrification process [41,44,49,50]. The presented behavior does not correspond to the trend identified by Lynn et al. [39] in which ash density increased with temperatures of up to 1000 °C. This may be due to differences in the equipment used for ash production, i.e. an electrical muffle instead of an incinerator.

Similarly, the Blaine fineness of the dried sewage sludge was reduced by calcination. Additionally, the rise of calcination temperature caused a decrease in the specific surface, as presented in Table 4. A higher fineness found in other studies [32,39,43] is achieved by the milling and/or sieving of the material, which contributes to the increase of the specific surface. In this study SSA has not been subjected to any process besides calcination, thus lower values of the specific surface are expected.

Fig. 1a presents the discrete and Fig. 1b presents the cumulative particle-size distribution, obtained by laser diffraction analysis. The D-values and mean diameters (D_{mean}) of materials are presented in Table 4. The particle-size of SSA ranged between 0.4 and 160 μm, with a D_{mean} of approximately 41.5 μm. Approximately 70% of particles were in the volume range of 11–80 μm.

The results evidenced that the calcination of sewage sludge reduced the particles size, as is indicated by the cumulative curves of ash samples (Fig. 1b). However, the mean diameter of ash samples increased with increasing temperature and exceeded the DSS diameter from 800 °C (Table 4). The discrete and cumulative curves of SSA600 and SSA700 are overlapped, indicating similar particle-size distributions. The curves also denote that these ashes are finer, followed by SSA800 and SSA900. This coincides with the Blaine fineness results.

X-ray diffraction was performed to identify the mineralogical composition of the ash. Diffractograms can be observed in Fig. 2. The results presented a heterogeneous composition consisting mainly of quartz (SiO_2), hematite (Fe_2O_3), albite ($Na(AlSi_3O_8)$), and microcline intermediate ($KAlSi_3O_8$). In addition, it was observed that calcite ($CaCO_3$) was only present in SSA600 as the thermal decomposition of this mineral starts at temperatures of approximately 700 °C. Thus, after calcination at higher temperatures, calcite decomposes into calcium oxide (CaO). Other minor compounds are muscovite ($KAl_3Si_3O_{10}(OH)_2$) and whitlockite ($Ca_{2.86}Mg_{0.14}(PO_4)_2$), which were identified at 900 °C.

Through the diffractograms, it was observed that the compounds identified by the X-ray diffraction agree with those presented by the chemical analysis. In addition, it has been noted that the ash samples are composed of crystalline phases with well-defined peaks. Part of silicon, which is the major element in the samples, is present in its crystalline phase and is identified as quartz. Fontes [27] suggests that the variation of quartz-peaks intensity with the calcination temperature of SSA is an indication of a modification in the crystalline structure by increasing temperature. The same behavior was observed by Wang [51]. The author states that, for one of the studied ash samples, quartz remained in crystalline phases at higher sintering temperatures (900 °C,

Table 3
Chemical composition in oxide content (%) of sewage sludge ash calcined at 600 °C (SSA600), 700 °C (SSA700), 800 °C (SSA800) and 900 °C (SSA900) samples.

Sample	SSA600	SSA700	SSA800	SSA900	Other SSA[a]			
					Mean	Min	Max	Deviation (δ)
Oxide	Mass content (%)							
SiO_2	43.64	44.99	46.83	49.02	31.95	16.60	56.10	10.29
Al_2O_3	16.85	17.20	18.92	16.34	14.05	5.10	28.65	5.69
Fe_2O_3	11.78	11.91	10.25	11.21	9.25	4.70	20.00	4.16
CaO	7.88	8.03	7.15	8.37	9.00	1.90	31.30	8.98
P_2O_5	6.62	7.07	6.24	6.86	8.01	1.67	17.75	5.03
MgO	2.63	2.25	2.61	2.30	2.00	0.82	3.93	0.88
K_2O	1.96	2.06	1.94	2.27	1.36	0.60	2.80	0.62
Na_2O	1.52	–	1.06	1.31	0.63	0.20	3.50	0.73
CuO	0.14	0.14	0.11	0.12	0.12	0.06	1.09	0.32
MnO	0.07	0.07	0.06	0.08	0.08	0.03	0.44	0.12
NiO	0.06	0.06	0.05	0.06	0.03	0.01	0.72	0.25
LOI	6.87	6.23	4.77	2.06	4.72	1.80	8.35	2.00

[a] [27,31,33–37,39,41,42,45–47].

Table 4
Particle size (D_{10}, D_{50}, D_{90}, D_{mean}), Blaine fineness, and density of sewage sludge ash calcined at 600 °C, 700 °C, 800 °C, and 900 °C samples.

Sample	SSA600	SSA700	SSA800	SSA900	Other SSA			
					Mean	Min	Max	Deviation (δ)
D_{10}	4.488	4.570	5.017	7.976	–	–	–	–
D_{50}	26.889	26.854	33.627	35.691	–	–	–	–
D_{90}	78.424	79.571	106.602	100.264	–	–	–	–
D_{mean}	34.839	35.172	47.728	48.384	–	–	–	–
Density (g/cm^3)	2.63	2.60	2.58	2.63	2.58[b]	2.06[b]	3.20[b]	0.25
Blaine fineness (m^2/kg)	644.40	562.20	406.93	340.89	658.42[c]	247.00[c]	1589.00[c]	537.93

[b] [19,27,34–36,40–45].
[c] [34–36,41,43].

1000 °C, and 1100 °C) and gradually increased in intensity. Thus, higher calcination temperatures have a greater tendency to crystallize the amorphous silica and, consequently, reduce the material amorphousness and pozzolanicity. Hematite appears in ashes calcined at 800 °C and 900 °C, resulting from the oxidation of iron.

3.2. Mortar compressive strength

Table 5 presents the mix proportions of mortars, as well as the water/binder ratios, the average flow diameter and the average compressive strength at day 7, obtained from specimens containing sewage sludge ash and metakaolin.

The results show that the compressive strength was reduced with increasing calcination temperatures. Only SSA600 and SSA700 could be classified as pozzolans, since their compressive strengths of 7.54 and 7.53 MPa, respectively, exceed the minimum of 6 MPa required by the Brazilian Standards [30]. The calcination temperature with a higher pozzolanic reaction (600 °C) was lower than expected, as other studies indicated that the ashes that calcined at 700 and 800 °C have higher pozzolanic activity [28,47,52]. This behavior may be a result of the lower content of amorphous silica found in SSA800 and SSA900 samples when compared to SSA600 and SSA700, as indicated by the diffractograms (Fig. 2) and the higher fineness of SSA600 and SSA700. As reported and consistent in the literature, metakaolin can be considered a pozzolan of high performance (18.28 MPa). This was confirmed by the results obtained from our test. In this method, it is noteworthy that the compressive strength obtained is mostly due to the pozzolanic effect of the material, since the strength is obtained through hydrated products resulting from the reaction between the calcium hydroxide and pozzolan. Thus, it was noted that some degree of pozzolanic reaction was present in all sewage sludge ash samples studied.

3.3. Electrical conductivity

From the conductivity curves in Fig. 3, it is observed that there was a decrease in electrical conductivity after the material insertion. This behavior is attributed to the CH fixation and consequent formation of insoluble products, which is an indication of pozzolanic potential. In the study of repeatability, data collected from five measurements were analyzed individually for each second, and some changes in electrical conductivity measurements for a given test was verified. The coefficient of variation (CV) was less than 3.5% for pozzolan/CH suspension and 13.5% in pozzolan aqueous solutions. The higher dispersion obtained by the last system was caused by the lower electrical conductivity achieved by the pozzolans in the water when compared to the calcium hydroxide solution. Because of this, the minor difference in conductivity that was reached in each measurement highly affects the CV. Nonetheless, the variation is considered acceptable, confirming the repeatability of this method. Table 6 presents the conductivity immediately before the material insertion (C_0), the absolute loss in conductivity after 100 s $(C_{poza})_{100}$ and 1000 s $(C_{poza})_{1000}$, the variation between initial and final conductivity (Δ_{100} and Δ_{1000}), and the relative loss in conductivity, $(\%LC)_{100}$ and $(\%LC)_{1000}$.

The relative loss in the conductivity curves for each material is shown in Fig. 4, which allows us to observe and compare the calcium hydroxide fixation by the samples. Regarding the sewage sludge ashes, the same tendency that was observed in the compressive strength test, where reactivity decreased as the calcination temperature increased, was verified. This indicates that the methodology may be applied successfully to compare the pozzolanic reaction of SSA. However, metakaolin diverged from the previous result, presenting only a relative loss in conductivity, which was only greater than SSA900. This may have been a result of the calcium hydroxide/pozzolan ratio used. Due to the

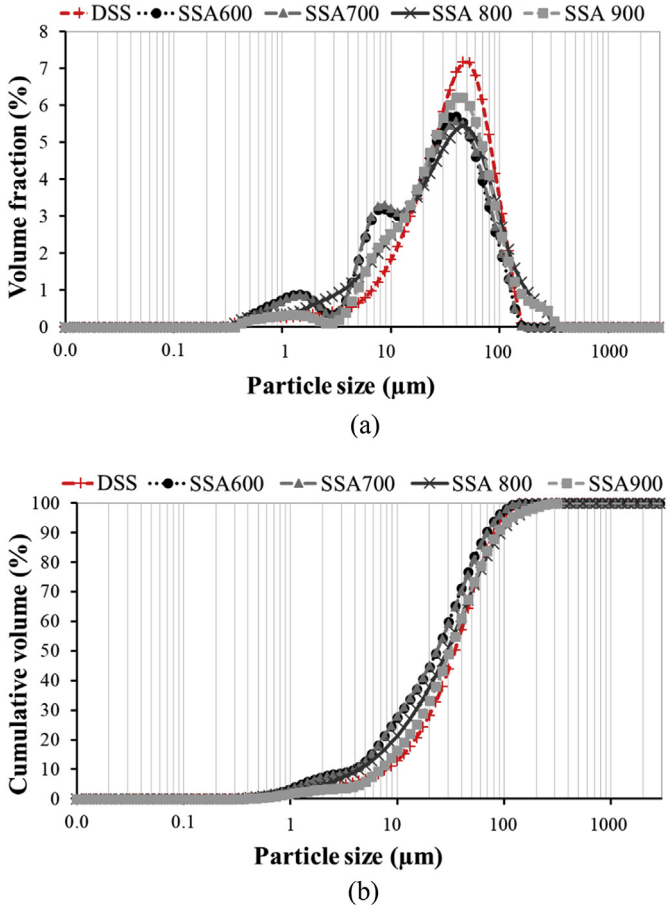

Fig. 1. (a) Discrete and (b) cumulative particle-size distribution of dry sewage sludge and sewage sludge ash es calcined at 600 °C, 700 °C, 800 °C, and 900 °C.

significant pozzolanicity, the metakaolin promoted a high consumption of CH in the first seconds of the test and distorted the results for the proposed method. Payá et al. [26] state that for highly reactive fly ashes, calcium hydroxide is consumed rapidly, and consequently, there would be no significant loss in conductivity over the remaining time. Therefore, a study of the influence of calcium hydroxide/metakaolin ratio would be necessary to determine the optimum amount of this pozzolan.

To identify the behavior of electrical conductivity over time, especially in the first seconds of the test, the conductivity curves are presented in a logarithmic scale in Fig. 5. Although Payá et al. [26] established 100, 1000, and 10000 s as periods of time at which the loss in conductivity should be verified in this study, the pattern exhibited by the curves of the sewage sludge ash was used to analyze the rate of consumption of calcium hydroxide. Three sections were observed: from 0 to 20 s, 20–200 s, and 200–1000 s. Thus, to determine the approximate reaction rate (R_S), the slope of each section of the conductivity curves was identified from linear regression and are listed in Table 7.

The rate of CH consumption was higher in the first section (from 0 to 20 s) than the following sections. Villar-Cocina et al. [23] have similarly verified a considerable loss in conductivity in early stages. During 20–200 s, the reaction was significantly reduced (2.6–5% of original speed). In section 3, the reaction remained practically the same as in section 2, decreasing slightly for SSA600 and SSA900, and increasing for SSA700 and SSA800. Although the main reactions occurred instantly after the pozzolan insertion, the remaining time contributed to defining the real pozzolanic potential of a material.

3.4. Comparison of obtained results and compressive strength test

The results of the compressive strength of the mortars at day 7 was related to the calcination temperature of the sewage sludge ash samples, as is presented in Fig. 6. The obtained graph shows that the compressive strength and calcination temperature tends to be a linear phenomenon. Thus, a higher temperature for ash calcination results in a mortar with a lower compressive resistance. Consequently, the increase

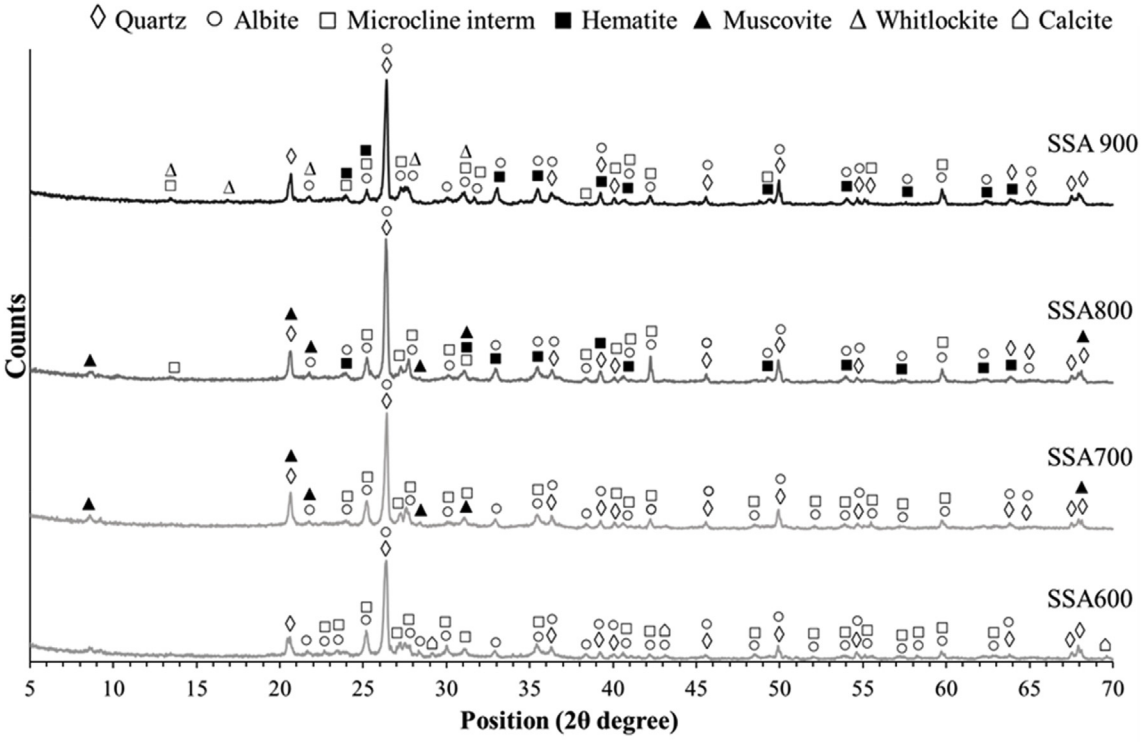

Fig. 2. X-ray diffraction traces of sewage sludge ashes calcined at 600 °C, 700 °C, 800 °C, and 900 °C.

Table 5
Mix proportions and compressive strength of sewage sludge ash calcined at 600 °C, 700 °C, 800 °C, 900 °C, and metakaolin mortar.

Specimens	Weight (g)				w/b	Average flow diameter (mm)	Compressive Strength (MPa)
	SSA	CH	Sand	Water			
SSA600	234.68	104.00	936.00	226.92	0.67	222.5	7.54
SSA700	232.00	104.00	936.00	221.76	0.66	217.5	7.53
SSA800	230.22	104.00	936.00	217.24	0.65	227.5	5.64
SSA900	234.68	104.00	936.00	220.14	0.65	229.5	3.71
MK	232.45	104.00	936.00	319.63	0.95	222.5	18.28

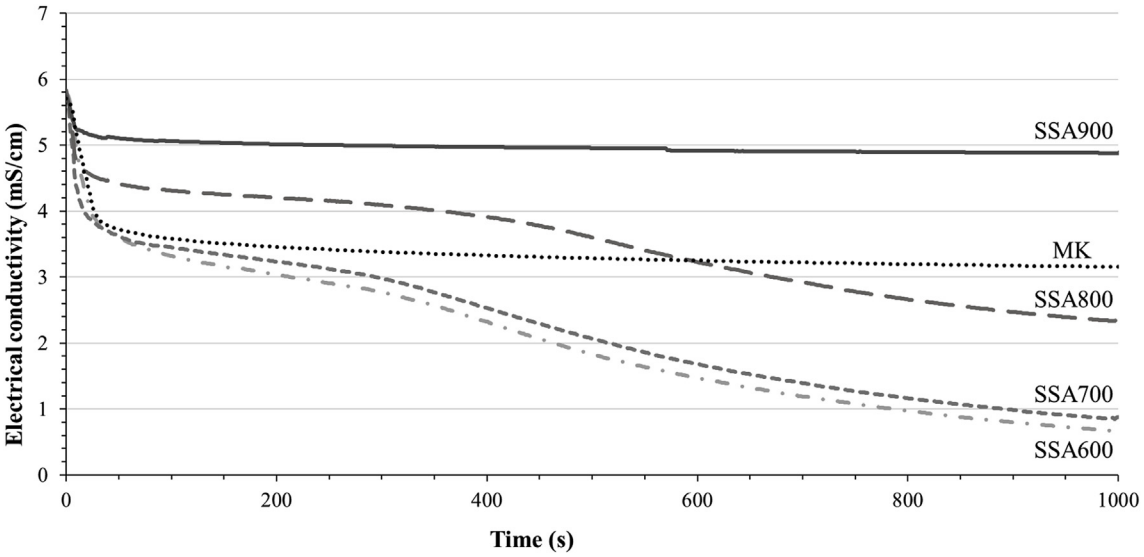

Fig. 3. Conductivity curves for sewage sludge ash calcined at 600 °C, 700 °C, 800 °C and 900 °C, and metakaolin in the 0–1000 s period.

Table 6
Electrical conductivity, variation of conductivity (Δ_t) and relative loss in conductivity (% LC) $_t$ for sewage sludge ash calcined at 600 °C, 700 °C, 800 °C and 900 °C, and metakaolin.

Sample	Conductivity (mS/cm)					$(\%LC)_{100}$	$(\%LC)_{1000}$
	C_0	$(C_{poza})_{100}$	Δ_{100}	$(C_{poza})_{1000}$	Δ_{1000}		
SSA600	5.783	3.317	2.47	0.676	5.11	42.65	88.30
SSA700	5.771	3.450	2.32	0.883	4.89	40.21	84.69
SSA800	5.826	4.310	1.52	2.380	3.45	26.03	59.14
SSA900	5.737	5.059	0.68	4.894	0.84	11.82	14.69
MK	5.705	3.582	2.12	3.166	2.54	37.22	44.51

in temperature promotes a reduction in the pozzolanic reactivity of SSA. According to the results from X-ray diffraction and laser granulometry, this behavior occurred due to a decrease in pozzolanicity caused by the increase of crystalline phases of silica and the mean diameter of particles. The same variation of silica's crystallinity as function of temperature was noticed in others supplementary cementitious materials [53–55], wherein higher temperatures conduct to convert amorphous silica to crystalline forms.

Fig. 7 shows the compressive strength at day 7 as a function of Blaine fineness. These parameters are directly proportional and also have a linear tendency. This demonstrates the importance of particle size distribution and specific surface area in SSA performance once these parameters directly affect the reaction between the calcium hydroxide and the pozzolan, as is indicated by Swamy [56], Pan [32], and Massaza [20]. The correlation had an opposite behavior to that presented in Fig. 6. This was due to the decrease in fineness caused by an increase in calcination temperature.

In Fig. 8, a significant correlation is observed between mortar compressive strength and the relative loss in conductivity. Thus, the tendency of this relationship is that the greater the relative loss of conductivity, the greater the compressive strength that is obtained by the mortars. Although the electrical conductivity test only evaluated SSA chemically, while the compressive strength test assessed both the chemical and physical contributions of the ash, the methods obtained similar results. This suggests that the proposed method is adequate to verify the performance of the sewage sludge ash.

4. Conclusions

The results of this study enable us to observe the influence of calcination temperature on the chemical, physical, and mineralogical characteristics of the ash obtained from a sewage sludge sample and to evaluate the possibility of using it as a supplementary cementitious material. Based on the literature, four calcination temperatures were defined to produce sewage sludge ash (SSA). In addition, metakaolin, a well-known mineral admixture, was used as a reference material.

The proposed method for pozzolanic reactivity evaluation by electrical conductivity presented an almost linear relationship with the test for determining pozzolanic activity by compressive strength. According to the results from both methods, SSA600 and SSA700 presented the highest pozzolanicity, followed by SSA800 and SSA900. This shows that the relative loss in conductivity is consistent with the consumption of CH and is sufficiently sensitive to compare and classify the pozzolanic reactivity of SSAs.

Through the electrical conductivity curves of the sewage sludge ashes, three sections were defined based on the reaction rate of CH consumption. The sections were characterized first by a period of rapid loss in conductivity (0–20 s), followed by a significant decrease in the reaction rate (20–200 s), and finally an increase or decrease in speed.

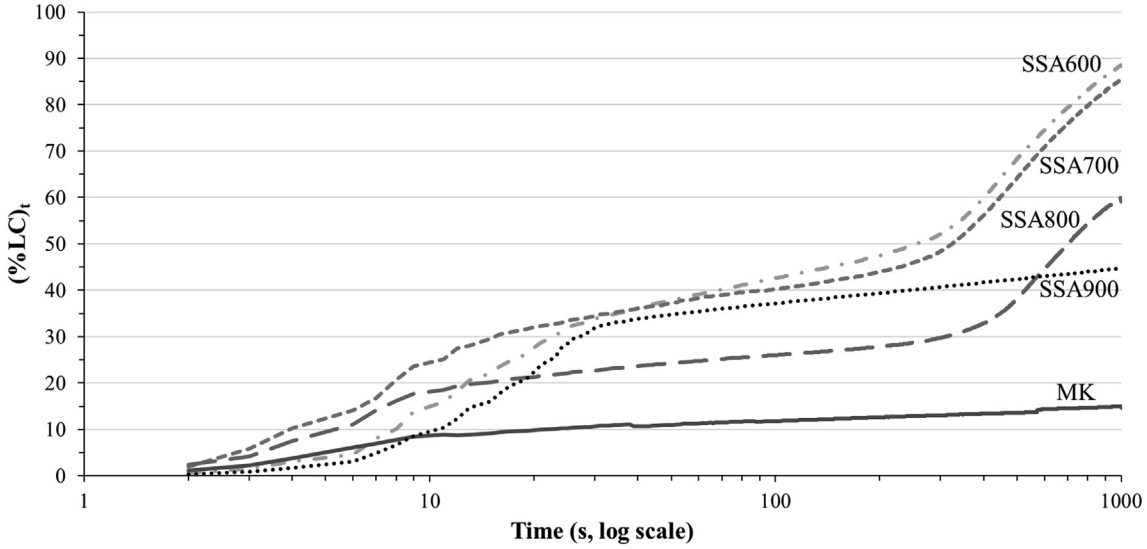

Fig. 4. Relative loss in conductivity for sewage sludge ashes calcined at 600, 700, 800, and 900 °C, and metakaolin.

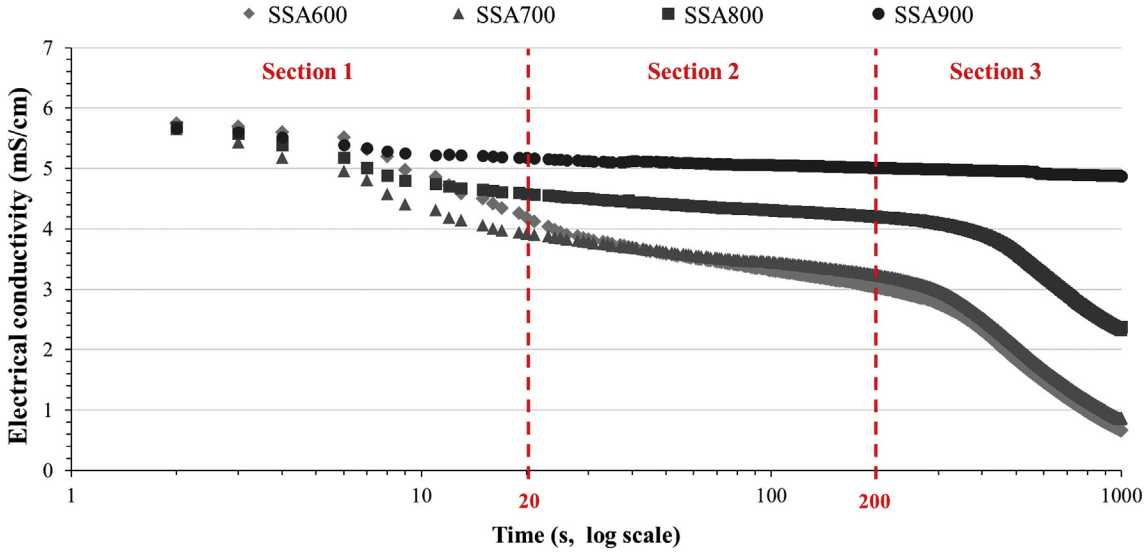

Fig. 5. Conductivity curves for sewage sludge ash calcined at 600 °C, 700 °C, 800 °C, 900 °C in log scale.

Table 7
Reaction rate for sewage sludge ash calcined at 600 °C, 700 °C, 800 °C, 900 °C at 0–20 s (R_1), 20–200 s (R_2), and 200–1000 s (R_3) periods.

Sample	Reaction rate (μS/cm/s)		
	R_1	R_2	R_3
SSA600	90.7	4.5	3.2
SSA700	92.3	3.0	3.2
SSA800	61.2	1.6	2.7
SSA900	27.4	0.7	0.2

Both SSA600 and SSA700, which had a higher specific surface area and a lower mean diameter, presented the highest losses in electrical conductivity and reached the minimum compressive strength required to be classified as a pozzolan. Moreover, these ash samples also had similar particle size distribution curves, indicating the substantial influence of fineness for the development of pozzolanic activity, as confirmed by the correlation presented in Fig. 7. The mineralogical analysis of SSAs indicated that the increase in the calcination temperature of ash may cause crystallization of amorphous silica in SSA, which is

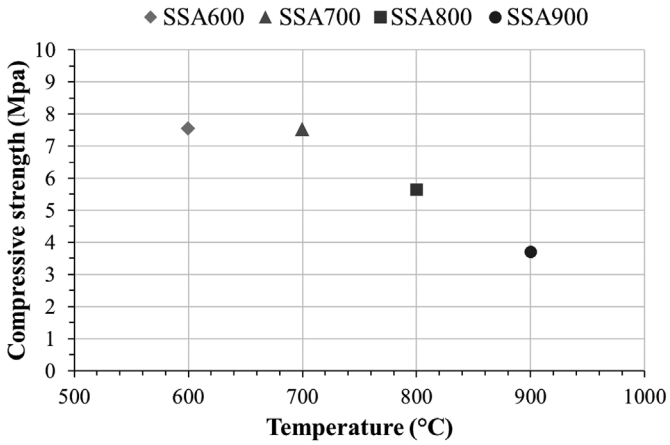

Fig. 6. Correlation between compressive strength at 7 days and temperature of calcination.

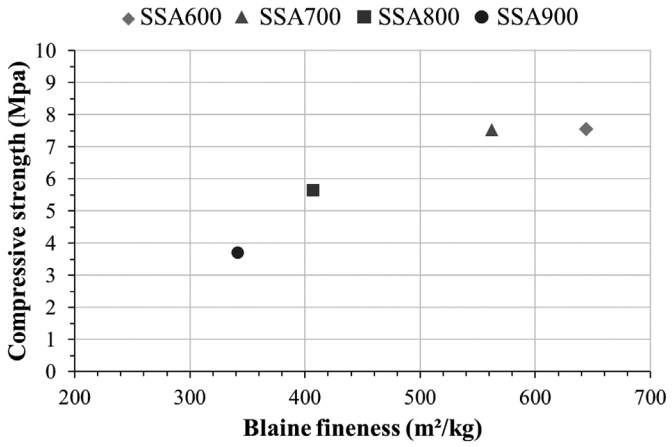

Fig. 7. Correlation between compressive strength at 7 days and Blaine fineness.

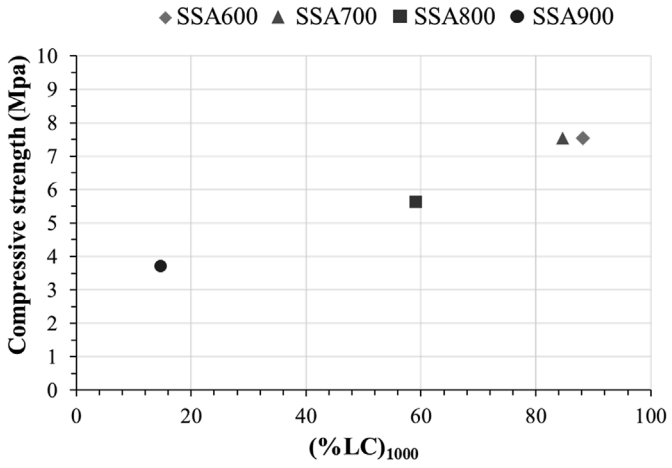

Fig. 8. Correlation between compressive strength at 7 days and relative loss in conductivity at 1000s.

correlated to the reduction of pozzolanic activity.

The calcination of sewage sludge at 600 °C was adequate to achieve a pozzolanic material for use in Portland cement mortar and concrete, promoting the recycling of a complex residue and contributing to the reduction of the amount of cement used in construction. Furthermore, the monitoring of pozzolanic reactivity by electrical conductivity is a quicker and simpler method for studying the reactivity of sewage sludge ash.

Acknowledgments

The authors wish to acknowledge the Foundation of Support to Science and Technology of Pernambuco (Facepe, process #IBPG-0579-3.01/15) and the National Council for Scientific and Technological Development (CNPq, process #140342/2018-4) for the scholarships conceded and the Institute of Technology of Pernambuco (ITEP) for providing infrastructure and support to perform part of the work reported here.

References

[1] The Cement Sustainability Initiative, Cement Industry Energy and CO_2 Performance: Getting the Numbers Right, GNR, 2016.
[2] R.M. Andrew, Global CO_2 emissions from cement production, Earth Syst. Sci. Data (2017) 1–52 https://doi.org/10.5194/essd-10-195-2018.
[3] Working Group III of the International Panel on Climate Change, IPCC Special Report on Carbon Dioxide Capture and Storage, Cambridge University Press, New Youk, 2005.
[4] R.K. Dhir, G.S. Ghataora, C.J. Lynn, R.K. Dhir, G.S. Ghataora, C.J. Lynn, 1 – introduction, Sustain. Constr. Mater (2017) 1–8, https://doi.org/10.1016/B978-0-08-100987-1.00001-9.
[5] Food and Agriculture Organization of the United Nations, AQUASTAT Produced and treated municipal wastewater, [Data File] http://www.fao.org/nr/water/aquastat/data/query/results.html, (2016) , Accessed date: 3 April 2019.
[6] United Nations Human Settlements Programme, Global Atlas of Excreta, Wastewater Sludge and Biossolids Management: Moving Foward the Sustainable and Welcome Uses of a Global Resource, Nairobi, (2008).
[7] Eurostat, Sewage sludge production and disposal, [Data File] http://appsso.eurostat.ec.europa.eu/nui/show.do?dataset=env_ww_spd&lang=en, (2016) , Accessed date: 3 April 2019.
[8] A.L.B. Geyer, Contribution to the Study of Final Disposal and Use of Sludge Ash from Sewage Treatment Plants as an Addition in Concrete (In Portuguese), Federal University of Rio Grande do Sul, 2001.
[9] C.V. Andreoli, M. von Sperling, F. Fernandes, Sludge Treatment and Disposal, IWA Publishing, London, 2007.
[10] M. Kacprzak, E. Neczaj, K. Fijałkowski, A. Grobelak, A. Grosser, M. Worwag, A. Rorat, H. Brattebo, Å. Almås, B.R. Singh, Sewage sludge disposal strategies for sustainable development, Environ. Res. 156 (2017) 39–46, https://doi.org/10.1016/j.envres.2017.03.010.
[11] C.V. Andreoli, Solid Waste from Sanitation: Processing, Recycling and Final Disposal, first ed., ABES, Rio de Janeiro, 2001 (in Portuguese), http://downloads.caixa.gov.br/_arquivos/desenvolvimento_urbano/saneamento/Residuos_solidos_saneamento.pdf.
[12] H. Kroiss, M. Zessner, Ecological and Economical Relevance of Sludge Treatment and Disposal Options, (2014), pp. 47–54.
[13] B.M. Cieślik, J. Namiešnik, P. Konieczka, Review of sewage sludge management: standards, regulations and analytical methods, J. Clean. Prod. 90 (2015) 1–15, https://doi.org/10.1016/j.jclepro.2014.11.031.
[14] S. Donatello, A. Freeman-Pask, M. Tyrer, C.R. Cheeseman, Effect of milling and acid washing on the pozzolanic activity of incinerator sewage sludge ash, Cement Concr. Compos. 32 (2010) 54–61, https://doi.org/10.1016/j.cemconcomp.2009.09.002.
[15] L.C. De Godoy, Logistics in disposal of sewage sludge (in Portuguese), Rev. Científica On-Line Tecnol. - Gestão - Humanismo. 2 (2013) 79–90.
[16] A.L. Castro, O.R. Silva, P.S. Scalize, Disposal scenario of sewage sludge: a review of papers published from 2004 to 2014 in Brazil, Multi-Sci. J. 1 (2015) 66–73.
[17] M. Smol, J. Kulczycka, A. Henclik, K. Gorazda, Z. Wzorek, The possible use of sewage sludge ash (SSA) in the construction industry as a way towards a circular economy, J. Clean. Prod. 95 (2015) 45–54, https://doi.org/10.1016/j.jclepro.2015.02.051.
[18] B.Q. Tempest, M.A. Pando, Characterization and demonstration of reuse applications of sewage sludge ash, Int. J. Geom. (2013) 552–559, https://doi.org/10.21660/2013.8.1620.
[19] T.D. Dyer, J.E. Halliday, R.K. Dhir, Hydration chemistry of sewage sludge ash used as a cement component, J. Mater. Civ. Eng. 23 (2011) 648–655, https://doi.org/10.1061/(ASCE)MT.1943-5533.0000221.
[20] F. Massazza, Pozzolanic cements, Cement Concr. Compos. 15 (1993) 185–214, https://doi.org/10.1016/0958-9465(93)90023-3.
[21] S. Donatello, C.R. Cheeseman, Recycling and recovery routes for incinerated sewage sludge ash (ISSA): a review, Waste Manag. 33 (2013) 2328–2340, https://doi.org/10.1016/j.wasman.2013.05.024.
[22] A.R. Pourkhorshidi, B. Hillemeier, M. Najimi, R. Herr, T. Parhizkar, A comparative study of the evaluation methods for pozzolans, Adv. Cem. Res. 22 (2010) 157–164, https://doi.org/10.1680/adcr.2010.22.3.157.
[23] E. Villar-Cociña, E. Valencia-Morales, R. González-Rodríguez, J. Hernández-Ruíz, Kinetics of the pozzolanic reaction between lime and sugar cane straw ash by electrical conductivity measurement: a kinetic-diffusive model, Cement Concr. Res. 33 (2003) 517–524, https://doi.org/10.1016/S0008-8846(02)00998-5.
[24] E. Raask, M.C. Bhaskar, Pozzolanic activity of pulverized fuel ash, Cement Concr. Res. 5 (1975) 363–375, https://doi.org/10.1016/0008-8846(75)90091-5.
[25] M.P. Luxán, F. Madruga, J. Saavedra, Rapid evaluation of pozzolanic activity of natural products by conductivity measurement, Cement Concr. Res. 19 (1989) 63–68, https://doi.org/10.1016/0008-8846(89)90066-5.
[26] J. Payá, M. Borrachero, J. Monzó, E. Peris-Mora, F. Amahjour, Enhanced conductivity measurement techniques for evaluation of fly ash pozzolanic activity, Cement Concr. Res. 31 (2001) 41–49, https://doi.org/10.1016/S0008-8846(00)00434-8.
[27] C.M.A. Fontes, Potential Use of the Sludge Ash from Sewage Treatment Plants as Supplementary Material in Concretes Production Using Portland Cements (In Portuguese), Federal University of Rio de Janeiro, 2003.
[28] S. Naamane, Z. Rais, M. Taleb, The effectiveness of the incineration of sewage sludge on the evolution of physicochemical and mechanical properties of Portland cement, Constr. Build. Mater. 112 (2016) 783–789, https://doi.org/10.1016/j.conbuildmat.2016.02.121.
[29] Associação Brasileira de Normas Técnicas, NBR 5751, Pozzolanic Materials - Determination of Pozzolanic Activity with Lime at Seven Days (In Portuguese), (2015).
[30] Associação Brasileira de Normas Técnicas, NBR 12653, Pozzolanic Materials - Requirements (In Portuguese), (2014).
[31] M.T. Pérez-Carrión, F. Baeza-Brotons, J. Payá, J.M. Saval, E. Zornoza, M.V. Borrachero, P. Garcés, Potential use of sewage sludge ash as a cement replacement in precast concrete blocks, Mater. Construcción 64 (2014) 1–7, https://doi.org/10.3989/mc.2014.06312.
[32] S.C. Pan, D.H. Tseng, C.C. Lee, C. Lee, Influence of the fineness of sewage sludge ash on the mortar properties, Cement Concr. Res. 33 (2003) 1749–1754, https://doi.org/10.1016/S0008-8846(03)00165-0.

[33] J. Monzó, J. Paya, M.V. Borrachero, A. Córcoles, Use of sewage sludge ash(SSA)-cement admixtures in mortars, Cement Concr. Res. 26 (1996) 1389–1398, https://doi.org/10.1016/0008-8846(96)00119-6.
[34] J.E. Halliday, M.R. Jones, T.D. Dyer, Ravindra K. Dhir, Potential use of UK sewage sludge ash in cement-based concrete, Proc. Inst. Civ. Eng. Waste Resour. Manag. 165 (2012) 57–66, https://doi.org/10.1680/warm.10.00039.
[35] M. Cyr, M. Coutand, P. Clastres, Technological and environmental behavior of sewage sludge ash (SSA) in cement-based materials, Cement Concr. Res. 37 (2007) 1278–1289, https://doi.org/10.1016/j.cemconres.2007.04.003.
[36] M. Coutand, M. Cyr, P. Clastres, Use of sewage sludge ash as mineral admixture in mortars, Proc. Inst. Civ. Eng. - Constr. Mater. 159 (2006) 153–162, https://doi.org/10.1680/coma.2006.159.4.153.
[37] E.G. Alcocel, P. Garcés, J.J. Martínez, J. Payá, L.G. Andión, Effect of sewage sludge ash (SSA) on the mechanical performance and corrosion levels of reinforced Portland cement mortars (in Spanish), Mater. Construcción 56 (2006) 31–43.
[38] S.C. Chin, D.S. Ing, A. Kusbiantoro, Y.K. Wong, S.W. Ahmad, Characterization of sewage sludge ASH (SSA) in cement mortar, ARPN J. Eng. Appl. Sci. 11 (2016) 2242–2247.
[39] C.J. Lynn, R.K. Dhir, G.S. Ghataora, R.P. West, Sewage sludge ash characteristics and potential for use in concrete, Constr. Build. Mater. 98 (2015) 767–779, https://doi.org/10.1016/j.conbuildmat.2015.08.122.
[40] J.F. de Lima, Evaluation of the Incorporation of Sewage Sludge Ash as a Mineral Admixture in Portland Cement Concrete (In Portuguese), Universidade Federal do Rio Grande do Norte, 2013.
[41] R.K. Dhir, G.S. Ghataora, C.J. Lynn, R.K. Dhir, G.S. Ghataora, C.J. Lynn, 4 – sewage sludge ash characteristics, Sustain. Constr. Mater. (2017) 69–110, https://doi.org/10.1016/B978-0-08-100987-1.00004-4.
[42] C.M.A. Fontes, Utilization of the Sewage Sludge and Urban Solid Waste Ashes in High Performance Concrete (In Portuguese), Universidade Federal do Rio de Janeiro, 2008, http://livros01.livrosgratis.com.br/cp069752.pdf.
[43] D.-H. Tseng, S.C. Pan, Enhancement of pozolanic activity and morphology of sewage sludge ash by calcination.pdf, J. Chin. Inst. Environ. Eng. 10 (2000) 261–270.
[44] D. Vouk, D. Nakic, N. Stirmer, C.R. Cheeseman, Use of sewage sludge ash in cementitious materials, Rev. Adv. Mater. Sci. 49 (2017) 158–170 http://findit.dtu.dk/catalog/2373165728?referrer=alert_mail.
[45] R.O. Yusuf, Z.Z. Noor, N.a. Moh, D.F. Moh, D. Din, A.H. Abba, Use of sewage sludge ash (SSA) in the production of cement and concrete - a review, Int. J. Glob Environ. Issues 12 (2012) 214, https://doi.org/10.1504/IJGENVI.2012.049382.
[46] M.M. Tashima, L. Reig, M.A. Santini, J.C. B Moraes, J.L. Akasaki, J. Payá, M.V. Borrachero, L. Soriano, Compressive strength and microstructure of alkali-activated blast furnace slag/sewage sludge ash (GGBS/SSA) blends cured at room temperature, Waste and Biomass Valorization 8 (2017) 1441–1451, https://doi.org/10.1007/s12649-016-9659-1.
[47] M.A. Tantawy, A.M. El-Roudi, E.M. Abdalla, M.A. Abdelzaher, Evaluation of the pozzolanic activity of sewage sludge ash, ISRN Chem. Eng. 2012 (2012) 1–8, https://doi.org/10.5402/2012/487037.
[48] W. Piasta, M. Lukawska, The effect of sewage sludge ash on properties of cement composites, Procedia Eng 161 (2016) 1018–1024, https://doi.org/10.1016/j.proeng.2016.08.842.
[49] K.L. Lin, K.Y. Chiang, D.F. Lin, Effect of heating temperature on the sintering characteristics of sewage sludge ash, J. Hazard Mater. 128 (2006) 175–181, https://doi.org/10.1016/j.jhazmat.2005.07.051.
[50] C.J. Lynn, R.K. Dhir, G.S. Ghataora, Sewage sludge ash characteristics and potential for use in bricks, tiles and glass ceramics, Water Sci. Technol. 74 (2016) 17–29, https://doi.org/10.2166/wst.2016.040.
[51] L. Wang, G. Skjevrak, J.E. Hustad, M.G. Grønli, Sintering characteristics of sewage sludge ashes at elevated temperatures, Fuel Process. Technol. 96 (2012) 88–97, https://doi.org/10.1016/j.fuproc.2011.12.022.
[52] G. Morales, Use of sanitary sewage sludge as raw material for the production of pozzolanic material (in Portuguese), Semin. Ci. Exatas/Tecnol. Londrina. 18/20 (1999) 39–45.
[53] V.P. Della, I. Kühn, D. Hotza, Rice husk ash as an alternate source for active silica production, Mater. Lett. 57 (2002) 818–821, https://doi.org/10.1016/S0167-577X(02)00879-0.
[54] J. Shen, X. Liu, S. Zhu, H. Zhang, J. Tan, Effects of calcination parameters on the silica phase of original and leached rice husk ash, Mater. Lett. 65 (2011) 1179–1183, https://doi.org/10.1016/j.matlet.2011.01.034.
[55] G.C. Cordeiro, R.D. Toledo Filho, E.M.R. Fairbairn, Effect of calcination temperature on the pozzolanic activity of sugar cane bagasse ash, Constr. Build. Mater. 23 (2009) 3301–3303, https://doi.org/10.1016/j.conbuildmat.2009.02.013.
[56] R.N. Swamy, Fly ash and slag: standards and specifications-help or hindrance? Mater. Struct. 26 (1993) 600–613, https://doi.org/10.1007/BF02472835.